

How to Recognize Cardiac Amyloidosis: Clinical Case Explanation

Kardiyak Amiloidoz Nasıl Tanınır? Klinik Vaka Açıklaması

ABSTRACT

Cardiac amyloidosis is a rare systemic condition characterized by the extracellular accumulation of amyloid proteins in the heart. These proteins can be deposited in various cardiac structures, including the valves, endocardium, myocardium, and pericardium. This abnormal protein deposition can disrupt normal heart function, leading to a range of symptoms and complications, such as heart failure, arrhythmias, and even sudden cardiac death. The diagnosis of cardiac amyloidosis is typically suspected based on characteristic clinical features, electrocardiogram abnormalities, and echocardiographic findings, which prompt further evaluation and confirmation. We present the case of a 57-year-old female hospitalized with significant exertional dyspnea, hypotension, lower extremity edema, and proteinuria. The aim of this case report is to enhance clinicians' understanding of this condition and to reduce the interval between symptom onset and diagnosis, thereby potentially improving the prognosis for affected patients.

Keywords: Amyloidosis, cardiovascular magnetic resonance, echocardiography, heart failure

ÖZET

Kardiyak Amiloidoz, kalp hücrelerinin dışına amiloid proteinlerinin birikmesiyle seyreden nadir görülen bir durumdur. Bu proteinler kalp kapakları, endokard, miyokard ve perikard gibi kalbin farklı bölgelerinde birikme eğilimindedir. Bu anormal protein birikimi, kalbin normal fonksiyonunu bozarak kalp yetmezliği, aritmiler ve hatta ani kalp ölümlerine neden olabilir. Kardiyak amiloidoz tanısı, ileri değerlendirme ve doğrulama gerektiren karakteristik bulgulara, elektrokardiyografi anormalliklerine ve ekokardiyografik özelliklere dayanarak şüphelenilir. Sunulan vakada, 57 yaşındaki bir kadın hasta ciddi efor dispnesi, hipotansiyon, alt ekstremitte ödemleri ve proteinüri semptomlarıyla hastanemize yatırılmıştır. Bu vaka sunumunun amacı, hekimlerin bu durumun farkındalığını artırmak, semptomların başlamasından teşhise kadar geçen süreyi azaltmak ve böylece hastaların prognozunu iyileştirmektir.

Anahtar Kelimeler: Amiloidoz, kardiyovasküler manyetik rezonans, ekokardiyografi, kalp yetmezliği

Amyloidosis is a rare disease characterized by the extracellular deposition of fibrillar proteins, which disrupt normal tissue architecture.¹ Amyloid deposits can affect multiple organs, including the heart, kidneys, liver, and gastrointestinal tract, with specific manifestations depending on the type of amyloidosis. Cardiac amyloidosis (CA) is notable for its rapid progression to heart failure.² The two most common types affecting the heart are immunoglobulin light chain amyloidosis (AL-CA) and transthyretin amyloidosis (ATTR). With an aging population, the prevalence of ATTR-CA is expected to rise. However, it is often underdiagnosed due to its slow progression and the non-specific nature of symptoms in older adults.³

Early and accurate identification of the CA subtype is essential for optimal patient management. Patients presenting with a hypertrophic cardiac pattern and heart failure with preserved ejection fraction (HFpEF), especially those who do not respond adequately to diuretic therapy, should be evaluated for infiltrative or storage diseases. CA is frequently diagnosed in this subset of patients.

Case Report

A 57-year-old woman was admitted to the clinic with significant weakness, hypotension, exertional dyspnea, and ankle swelling. She had been receiving optimal

CASE REPORT OLGU SUNUMU

Shafag Mustafaeva¹ 

Uzeyir Rahimov¹ 

Emin Karimli¹ 

Khatira Abdulalimova¹ 

Shahla Shabanova² 

¹Department of Cardiology, Baku Medical Plaza, Baku, Azerbaijan

²Department of Internal Medicine, Azerbaijan Medical University, Baku, Azerbaijan

Corresponding author:

Emin Karimli
✉ dr.karimli.emin@gmail.com

Received: July 21, 2024

Accepted: October 03, 2024

Cite this article as: Mustafaeva S, Rahimov U, Karimli E, Abdulalimova K, Shabanova S. How to Recognize Cardiac Amyloidosis: Clinical Case Explanation. *Türk Kardiyol Dern Ars.* 2025;53(4):000-000.

DOI: 10.5543/tkda.2024.79810



Available online at archivestsc.com.
Content of this journal is licensed under a Creative Commons Attribution - NonCommercial-NoDerivatives 4.0 International License.

medical therapy for congestive heart failure for the past two years, but her symptoms had progressively worsened over the previous three months (New York Heart Association (NYHA) Functional Classification Class III to IV). A chest X-ray revealed massive bilateral pleural effusion, necessitating pleural drainage on both sides. Despite high-dose loop diuretic therapy during this period, peripheral edema persisted. Auscultation revealed absent breath sounds bilaterally at the lung bases, arrhythmic heart sounds, and a midsystolic murmur in the mitral area. Her blood pressure was 90/55 mmHg, pulse rate 85 beats per minute, and oxygen saturation was 94% on room air.

The electrocardiogram (ECG) showed low-voltage QRS complexes in the limb leads and atrial fibrillation (Figure 1). Transthoracic echocardiography (TTE) revealed mildly reduced left ventricular ejection fraction (LVEF = 50%), concentric left ventricular hypertrophy, particularly of the interventricular septum (IVS 16 mm), with the characteristic "granular sparkling" appearance of the myocardium (Figure 2A-C, Video). Additional findings included biatrial enlargement, grade III diastolic dysfunction (Figure 2D-E), increased right ventricular wall thickness (Figure 2F), elevated systolic pulmonary arterial pressure (45 mmHg), and a small pericardial effusion surrounding both ventricles (Figure 2A-C). Due to the inadequate response

ABBREVIATIONS

AL-CA	Light chain amyloidosis
ATTR	Transthyretin amyloidosis
CA	Cardiac amyloidosis
ECV	Extracellular volume
HFpEF	Heart failure with preserved ejection fraction
LV	Left ventricle
LVEDV	Left ventricular end-diastolic volume
LVEF	Left ventricular ejection fraction
MRI	Magnetic resonance imaging
NYHA	New York Heart Association
RV	Right ventricular
TTE	Transthoracic echocardiography

to diuretic therapy over three months, persistent bilateral pleural effusion, and marked shortness of breath, a thoracic computed tomography (CT) scan was performed. The CT confirmed bilateral pleural effusion (Figure 3). Laboratory analysis showed elevated N-terminal pro-B-type natriuretic peptide (NT-proBNP) (21,264 pg/mL; upper limit of normal: 225 pg/mL) and cardiac troponin I (514 ng/L; upper limit of normal: 19.8 ng/L). Total serum protein was low at 49.8 g/L



Figure 1. Electrocardiography.

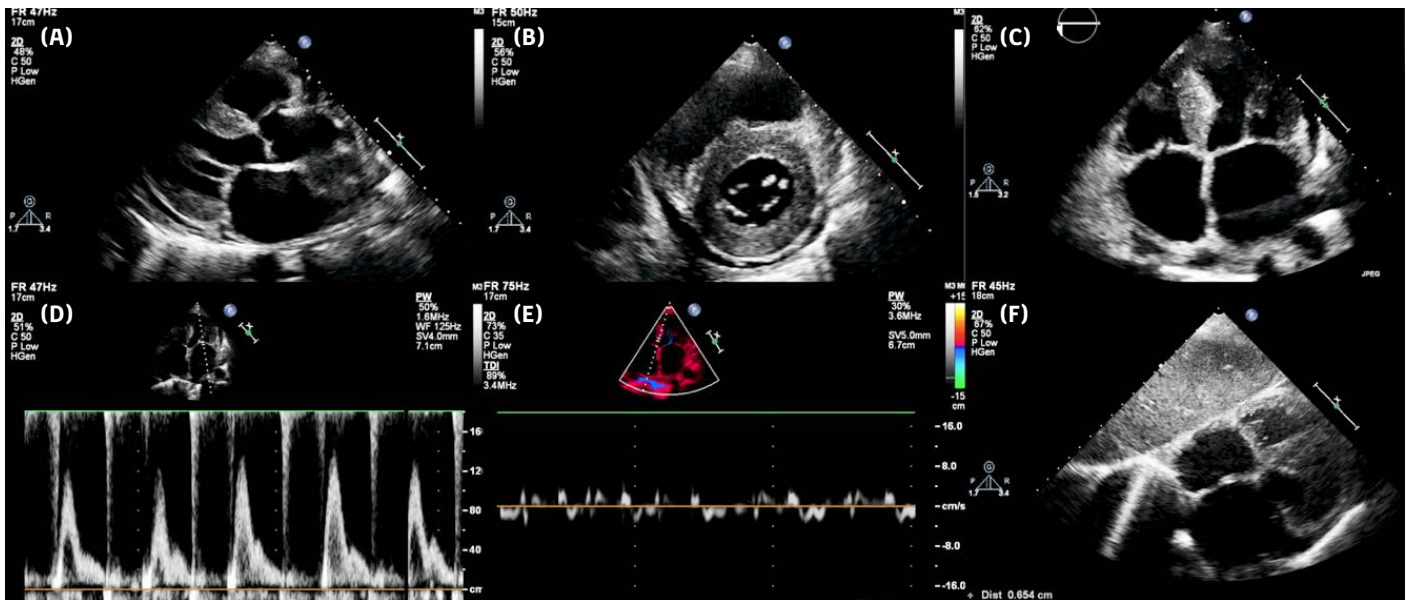


Figure 2. Echocardiography: (A) Parasternal long-axis view; (B) Parasternal short-axis view; (C) Apical four-chamber view; (D) Mitral inflow velocities; (E) Tissue doppler velocities; (F) Subcostal view.



Figure 3. Computed tomography.

(normal lower limit: 64 g/L), and albumin was 2.2 g/dL (normal lower limit: 3.4 g/dL). Urine analysis revealed proteinuria (0.9 g/L). Other blood test results were within normal limits.

To clarify the etiology of the hypertrophied left ventricle (LV), the patient was referred for cardiac magnetic resonance imaging (MRI). MRI revealed predominant LV hypertrophy at the septal wall (17 mm) and mildly reduced LV systolic function (LVEF = 42%, left ventricular end-diastolic volume [LVEDV] = 56 mL/m², left ventricular end-systolic volume [LVESV] = 32 mL/m²). Right ventricular (RV) wall thickness measured 6 mm. Mild biatrial dilatation was noted, along with the presence of fat tissue exhibiting a lipomatous appearance in the interatrial septum (IAS, 16 mm), a suggestive sign of CA (Figure 4A). A circumferential pericardial effusion with a thickness of up to 10 mm was also observed. Following gadolinium administration, patchy enhancement patterns

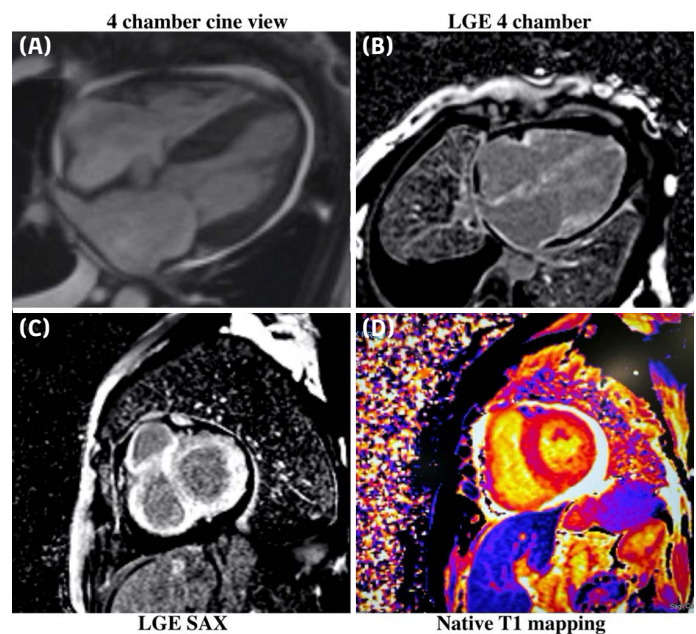


Figure 4. Cardiac magnetic resonance imaging (MRI): (A) Apical four-chamber cine view; (B) Apical four-chamber late gadolinium enhancement (LGE) view; (C) Left ventricular (LV) short-axis late gadolinium enhancement (LGE) view; (D) Native T1 mapping.

were seen, with diffuse subendocardial and transmural involvement across all four chambers, including the interatrial septum (Figure 4B-C). Elevated native T1 mapping values (T1 mapping 1233 ms vs. reference 1040 ms) and increased extracellular volume (ECV, 37%) indicated extensive fibrosis (Figure 4D). These findings confirmed the diagnosis of CA. The patient was subsequently referred to a hematologist for further evaluation.

A bone marrow biopsy revealed hypercellularity with an increased count of kappa monotypic plasma cells and Congo red dye positivity, characteristic of amyloidosis. Multiple myeloma was ruled out due to normal blood immunoglobulin levels. Monoclonal light chains were detected in both serum and 24-hour urine samples by immunofixation electrophoresis: kappa chains were 3.07 g/L (normal range: 1.3-3.7 g/L) and lambda chains were 0.7 g/L (normal range: 0.93-2.42 mg/L). The kappa-to-lambda ratio was 4.20 (normal range: 1.17-2.93). An abnormal kappa-lambda ratio is observed in more than 90% of untreated cases of AL-CA. Based on these findings, the final diagnosis was light chain amyloidosis.

Following diagnosis, the patient was started on VRD therapy (bortezomib, lenalidomide, dexamethasone), along with supportive treatments including spironolactone, furosemide, rivaroxaban, and empagliflozin. Despite the initial chemotherapy sessions, clinical improvement was limited. Troponin I decreased to 398 ng/L and NT-proBNP to 19,789 pg/mL. Unfortunately, after three months of treatment, the patient showed no significant clinical improvement, likely due to the advanced stage of disease at the time of diagnosis. The patient passed away in the fourth month of treatment.

Discussion

In AL amyloidosis, cardiac involvement occurs in up to 75% of cases.^{3,4} AL-CA typically manifests after the age of 40 and shows no gender predisposition, whereas ATTR CA generally affects individuals over 65 years of age.⁵ Median survival following diagnosis is approximately 24 months in AL-CA, compared to 31-69 months in ATTR amyloidosis. The presence of heart failure is associated with a poor prognosis, with a median survival of just six months, as seen in our case.⁶ Due to its rarity and overlapping clinical features with other conditions such as chronic renal failure, hypertension, and hypertrophic cardiomyopathy, diagnosis of CA is often delayed, with an average diagnostic delay of around two years.

Recent advances in treatment have emphasized the importance of early diagnosis. Clinicians should be familiar with the diagnostic algorithm for CA to facilitate timely recognition. For example, patients with HFpEF who are refractory to diuretics should be evaluated for potential infiltrative or storage diseases, including CA. Diagnostic suspicion should be heightened in patients with LV wall thickening (>1 2 mm) and at least one associated 'red flag' symptom (Table 1).⁶ Although our patient exhibited classic signs of AL-CA, achieving an early diagnosis remained a challenge.

ECG is a simple and routine diagnostic tool. In amyloidosis, typical ECG findings may include low-voltage ECG, a pseudoinfarction pattern, or atrial fibrillation. The next step in evaluation is TTE.

Basic and essential imaging techniques such as TTE are pivotal for both diagnosis and management. TTE serves as a fundamental tool, with characteristic features including biatrial enlargement, small hypertrophied ventricles, and pericardial effusion, findings suggestive of CA. LV wall thickening and a "speckled" myocardial appearance often indicate amyloid infiltration.⁷ Marked LV hypertrophy (> 18 mm) tends to favor ATTR amyloidosis over AL amyloidosis.⁸ LV systolic function is typically preserved or

Table 1. Red Flags of Cardiac Amyloidosis

Red Flags	Presented in current patient
Heart failure	Yes
Aortic stenosis in ≥ 65 years	-
Hypotension or normotensive if previously hypertensive	Yes
Nephrotic syndrome	Yes
Peripheral or autonomic neuropathy	-
Bilateral carpal tunnel syndrome	-
Ruptured biceps tendon	-
Periorbital purpura	-
Decreased QRS voltage to mass ratio	Yes
Pseudo Q waves on ECG	-
Reduced longitudinal strain with apical sparing	-
Subendocardial/transmural LGE or increased ECV	Yes

ECG, Electrocardiogram; LGE, Late gadolinium enhancement; ECV, Extracellular volume.

only mildly reduced. However, impaired global longitudinal strain parameters of the LV can be detected in early stages of the disease. An apical "sparing" pattern, specific to CA, may also be evident early on, along with diastolic dysfunction characterized by restrictive physiology.

In the presence of LV hypertrophy and a restrictive diastolic dysfunction pattern, cardiac MRI plays a key role in further tissue characterization. CA MRI is also valuable for monitoring treatment response in CA.⁹ Late gadolinium enhancement (LGE) plays an important role in the diagnosis of CA. On LGE images, despite optimal imaging techniques, achieving proper myocardial nulling can be challenging. In CA, complete nulling of the myocardium occurs before the blood pool—an abnormal finding, as normally the myocardium nulls after the blood pool. This pattern has a high sensitivity (100%) and is strongly indicative of CA.¹⁰ An increase in both native myocardial T1 relaxation time and ECV are also important diagnostic markers for CA.^{11,12} The accumulation of amyloid fibrils in the myocardium leads to a diffusely increased ECV. As in our patient, diffuse hyperenhancement not only identifies cardiac involvement but also serves as a strong predictor of mortality.¹³ The characteristic LGE pattern in CA is diffuse subendocardial enhancement, which has a specificity of 95%.¹⁴ In some cases, diffuse transmural LGE may also be observed, typically in more advanced stages of the disease, and is associated with a particularly poor prognosis. The average 24-month survival rate is approximately 60% in patients with transmural enhancement, compared to 80% in those with subendocardial enhancement.¹⁵ Our patient exhibited both transmural and subendocardial LGE involving all four cardiac chambers. Unfortunately, she survived only four months following diagnosis.

The findings for each form of amyloidosis vary depending on associated symptoms and diagnostic criteria. The most common symptoms of AL-CA include congestive heart

failure accompanied by nephrotic syndrome, macroglossia, orthostatic hypotension, and periorbital purpura (commonly referred to as "raccoon eyes"). In contrast, ATTR amyloidosis is more frequently observed in older adults (> 65 years) and is often associated with new-onset aortic stenosis, a history of carpal tunnel syndrome, or spinal stenosis. According to some studies, amyloid deposits in the ligamentum flavum have been found in approximately 40% of patients with lumbar spinal stenosis.¹⁶ Studies indicate that low-voltage waveforms on ECG are more prevalent in the AL subtype compared to the ATTR subtype, although a pseudoinfarction pattern may be present in both. On TTE, concentric LV hypertrophy is more common in AL-CA, whereas eccentric LV hypertrophy is more typical of ATTR. Marked LV hypertrophy (> 18 mm) tends to favor a diagnosis of ATTR over AL amyloidosis. On cardiac MRI, diffuse transmural LGE is more commonly seen in ATTR amyloidosis compared to AL.

Based on the above diagnostic findings, CA was suspected. The next diagnostic step is to detect monoclonal light chains in the serum and 24-hour urine using immunofixation electrophoresis. The presence of monoclonal light chains in both serum and urine is indicative of AL-CA. In such cases, a biopsy of the involved organ is preferred to confirm the diagnosis. If no monoclonal proteins are detected in serum and urine, ATTR CA is more likely, and the subsequent step is to perform technetium-99m pyrophosphate ((99m)Tc-PYP) scintigraphy.

Endomyocardial biopsy is an invasive procedure that requires technical expertise and carries a risk of complications. In contrast, specific staining of bone marrow biopsy plays a crucial role in diagnosing AL-CA. Tissues stained with Congo red for amyloid appear pink and exhibit yellow-green birefringence under polarized light.¹⁷

In our case, the patient first underwent serum and urine immunofixation electrophoresis to detect monoclonal light chains (kappa and lambda). Given the extended turnaround time for these results (at least 10 days) and the patient's critical condition, we decided to perform a bone marrow biopsy simultaneously, based on the clinical presentation, non-invasive diagnostic findings, and a high probability of AL-CA, to expedite the diagnostic process.

Biomarkers such as troponin I and NT-proBNP play critical roles in both the diagnosis and prognosis of CA. In our case, NT-proBNP levels exceeding 8,500 ng/L indicated a very poor prognosis.^{18,19}

Treatment of CA is complex and must be tailored to the specific amyloid type. Hypotension, which is especially common in AL-CA, often complicates standard heart failure therapies and requires careful management to avoid worsening hypotension. In advanced stages, beta-blockers are typically avoided, and treatment focuses on maintaining adequate cardiac output using diuretics and sodium-glucose co-transporter 2 (SGLT2) inhibitors.²⁰ The cornerstone of AL-CA treatment involves suppressing light chain production and promoting amyloid clearance, most commonly achieved through a regimen of cyclophosphamide, bortezomib, and dexamethasone (CyBorD).²¹

Diagnostic algorithm for cardiac amyloidosis is illustrated in Figure 5.

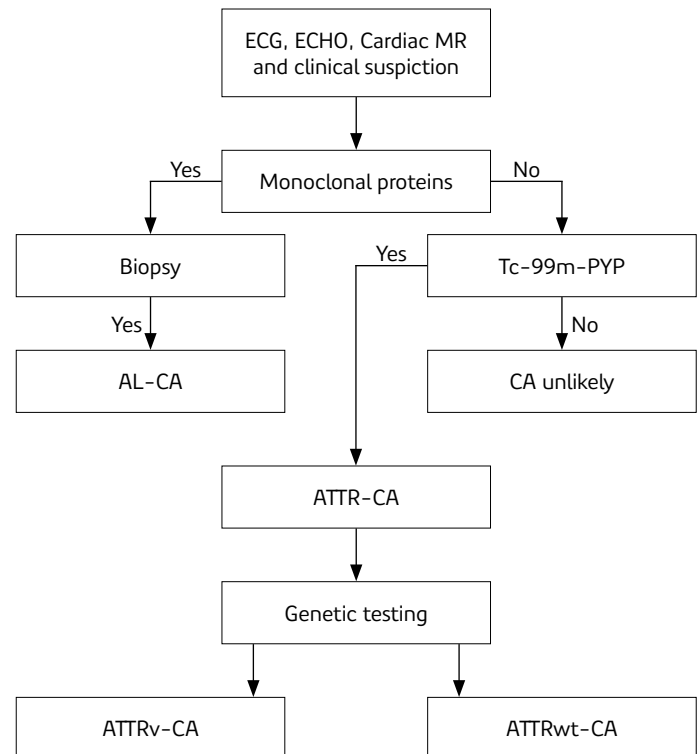


Figure 5. Diagnostic Algorithm for Cardiac Amyloidosis.

Conclusion

AL amyloidosis represents the most aggressive form of amyloidosis, particularly when diagnosed at an advanced stage. In our case, AL-CA presented with severe heart failure and extensive fibrosis involving all cardiac chambers, and was associated with a poor prognosis, with survival limited to six months. Amyloidosis remains a challenging condition to detect, often taking years from symptom onset to diagnosis. This clinical case underscores the importance of raising awareness among clinicians about this debilitating disease.

It is imperative to consider CA in patients with heart failure with preserved ejection fraction who are resistant to conventional therapies. Additionally, the presence of low-voltage findings on ECG combined with unexplained LV hypertrophy should raise suspicion of amyloidosis. Recognizing the "red flags" associated with the disease, such as elevated biomarker levels (NT-proBNP, troponin I), is essential for early diagnosis.

Non-invasive imaging modalities, including TTE and cardiac MRI, play pivotal roles in diagnosing CA, assessing disease severity, and guiding therapeutic strategies. Early identification and accurate classification of the amyloidosis subtype are critical for optimizing patient outcomes and implementing individualized treatment plans.

Ethics Committee Approval: This is a single case report, and therefore ethics committee approval was not required in accordance with institutional policies.

Informed Consent: Written informed consent was obtained from the participant for publication of this case.

Conflict of Interest: The authors have no conflicts of interest to declare.

Funding: The authors declared that this study received no financial support.

Use of AI for Writing Assistance: Artificial intelligence (AI)-assisted technologies were not used in the preparation of this submitted work.

Author Contributions: Concept – S.M.; Design – S.M., E.K.; Supervision – U.R., E.K.; Resource – S.M.; Materials – S.M., K.A.; Data Collection and/or Processing – S.M.; Analysis and/or Interpretation – S.M., K.A., S.S.; Literature Review – S.M., K.A., S.S.; Writing – S.M., E.K., K.A.; Critical Review – E.K., S.S.

Peer-review: Externally peer-reviewed.

Video 1. Echocardiography: Apical 4 chamber view.

References

1. Rapezzi C, Merlini G, Quarta CC, et al. Systemic cardiac amyloidoses: Disease profiles and clinical courses of the 3 main types. *Circulation*. 2009;120(13):1203–1212. [\[CrossRef\]](#)
2. Dubrey SW, Hawkins PN, Falk RH. Amyloid diseases of the heart: Assessment, diagnosis, and referral. *Heart*. 2011;97(1):75–84. [\[CrossRef\]](#)
3. Dorbala S, Ando Y, Bokhari S, et al. ASNC/AHA/ASE/EANM/HFSA/ISA/SCMR/SNMMI expert consensus recommendations for multimodality imaging in cardiac amyloidosis: Part 1 of 2-evidence base and standardized methods of imaging. *J Nucl Cardiol*. 2019;26(6):2065–2123. Erratum in: *J Nucl Cardiol*. 2021;28(4):1761–1762. [\[CrossRef\]](#)
4. Writing Committee; Kittleson MM, Ruberg FL, Ambardekar AV, et al. 2023 ACC Expert consensus decision pathway on comprehensive multidisciplinary care for the patient with cardiac amyloidosis: A report of the American College of Cardiology Solution Set Oversight Committee. *J Am Coll Cardiol*. 2023;81(11):1076–1126. Erratum in: *J Am Coll Cardiol*. 2023;81(11):1135. [\[CrossRef\]](#)
5. Maleszewski JJ. Cardiac amyloidosis: Pathology, nomenclature, and typing. *Cardiovasc Pathol*. 2015;24(6):343–350. [\[CrossRef\]](#)
6. Garcia-Pavia P, Rapezzi C, Adler Y, et al. Diagnosis and treatment of cardiac amyloidosis: A position statement of the ESC Working Group on Myocardial and Pericardial Diseases. *Eur Heart J*. 2021;42(16):1554–1568. [\[CrossRef\]](#)
7. Falk RH, Quarta CC. Echocardiography in cardiac amyloidosis. *Heart Fail Rev*. 2015;20(2):125–131. [\[CrossRef\]](#)
8. Falk RH, Alexander KM, Liao R, Dorbala S. AL (Light-Chain) cardiac amyloidosis: A review of diagnosis and therapy. *J Am Coll Cardiol*. 2016;68(12):1323–1341. [\[CrossRef\]](#)
9. Martinez-Naharro A, Hawkins PN, Fontana M. Cardiac amyloidosis. *Clin Med (Lond)*. 2018;18(Suppl 2):s30–s35. [\[CrossRef\]](#)
10. White JA, Kim HW, Shah D, et al. CMR imaging with rapid visual T1 assessment predicts mortality in patients suspected of cardiac amyloidosis. *JACC Cardiovasc Imaging*. 2014;7(2):143–156. [\[CrossRef\]](#)
11. Duca F, Kammerlander AA, Panzenböck A, et al. Cardiac magnetic resonance T1 mapping in cardiac amyloidosis. *JACC Cardiovasc Imaging*. 2018;11(12):1924–1926. [\[CrossRef\]](#)
12. Banyersad SM, Sado DM, Flett AS, et al. Quantification of myocardial extracellular volume fraction in systemic AL amyloidosis: An equilibrium contrast cardiovascular magnetic resonance study. *Circ Cardiovasc Imaging*. 2013;6(1):34–39. [\[CrossRef\]](#)
13. White JA, Kim HW, Shah D, et al. CMR imaging with rapid visual T1 assessment predicts mortality in patients suspected of cardiac amyloidosis. *JACC Cardiovasc Imaging*. 2014;7(2):143–156. [\[CrossRef\]](#)
14. Carvalho FP, Erthal F, Azevedo CF. The role of cardiac MR imaging in the assessment of patients with cardiac amyloidosis. *Magn Reson Imaging Clin N Am*. 2019;27(3):453–463. [\[CrossRef\]](#)
15. Fontana M, Pica S, Reant P, et al. Prognostic value of late gadolinium enhancement cardiovascular magnetic resonance in cardiac amyloidosis. *Circulation*. 2015;132(16):1570–1579. [\[CrossRef\]](#)
16. Yanagisawa A, Ueda M, Sueyoshi T, et al. Amyloid deposits derived from transthyretin in the ligamentum flavum as related to lumbar spinal canal stenosis. *Mod Pathol*. 2015;28(2):201–207. [\[CrossRef\]](#)
17. Hassan W, Al-Sergani H, Mourad W, Tabbaa R. Amyloid heart disease. New frontiers and insights in pathophysiology, diagnosis, and management. *Tex Heart Inst J*. 2005;32(2):178–184.
18. Richards DB, Cookson LM, Berges AC, et al. Therapeutic clearance of amyloid by antibodies to serum amyloid p component. *N Engl J Med*. 2015;373(12):1106–1114. [\[CrossRef\]](#)
19. Wechalekar AD, Schonland SO, Kastiris E, et al. A European collaborative study of treatment outcomes in 346 patients with cardiac stage III AL amyloidosis. *Blood*. 2013;121(17):3420–3427. [\[CrossRef\]](#)
20. Adam RD, Coriu D, Jercan A, et al. Progress and challenges in the treatment of cardiac amyloidosis: A review of the literature. *ESC Heart Fail*. 2021;8(4):2380–2396. [\[CrossRef\]](#)
21. Mikhael JR, Schuster SR, Jimenez-Zepeda VH, et al. Cyclophosphamide-bortezomib-dexamethasone (CyBorD) produces rapid and complete hematologic response in patients with AL amyloidosis. *Blood*. 2012;119(19):4391–4394. [\[CrossRef\]](#)